

Featured Article

The Na⁺/I⁻ Symporter Mediates Iodide Uptake in Breast Cancer Metastases and Can Be Selectively Down-Regulated in the Thyroid

Irene L. Wapnir,¹ Michael Goris,²
Anthony Yudd,⁴ Orsolya Dohan,⁵
Donna Adelman,¹ Kent Nowels,³ and
Nancy Carrasco⁵

¹Department of Surgery, ²Division of Nuclear Medicine, and ³Department of Pathology, Stanford University School of Medicine, Stanford, California; ⁴Department of Radiology, University of Medicine and Dentistry of New Jersey, Robert Wood Johnson Medical School, New Brunswick, New Jersey; and ⁵Department of Molecular Pharmacology, Albert Einstein College of Medicine, Bronx, New York

ABSTRACT

Purpose: The Na⁺/I⁻ symporter (NIS) is a key plasma membrane protein that mediates active iodide (I⁻) transport in the thyroid, lactating breast, and other tissues. Functional NIS expression in thyroid cancer accounts for the longstanding success of radioactive iodide (¹³¹I) ablation of metastases after thyroidectomy. Breast cancer is the only other cancer demonstrating endogenous functional NIS expression. Until now, NIS activity in breast cancer metastases (BCM) was unproven.

Experimental Design: Twenty-seven women were scanned with ^{99m}TcO₄⁻ or ¹²³I⁻ to assess NIS activity in their metastases. An ¹³¹I dosimetry study was offered to patients with I⁻-accumulating tumors. Selective down-regulation of thyroid NIS was tested in 13 patients with T₃ and in one case with T₃ + methimazole (MMI; blocks I⁻ organification). NIS expression was evaluated in index and/or metastatic tumor samples by immunohistochemistry.

Results: I⁻ uptake was noted in 25% of NIS-expressing tumors (two of eight). The remaining cases did not show NIS expression or activity. Thyroid I⁻ uptakes were decreased to ≤2.8% at 24 h in T₃-treated patients and 1/100 normal with T₃/MMI. Uptake (2.9%) was calculated in a peribronchial metastasis on ¹³¹I dosimetry scans at 4 h with disappearance of the signal by 24 h. We estimated a therapeutic dose of 3000 cGy could be achieved in this metastasis with 100 mCi

of ¹³¹I if the tumor exhibited the same dynamics as the T₃/MMI-suppressed thyroid.

Conclusions: This is the first article of *in vivo*, scintigraphically detected, NIS-mediated I⁻ accumulation in human BCM. T₃/MMI down-regulation of thyroid NIS makes ¹³¹I-radioablation of BCM possible with negligible thyroid uptake and radiation damage.

INTRODUCTION

For the better part of the 20th century, mastectomy was the sole treatment offered women with breast cancer. Today, neo-adjuvant and adjuvant systemic therapies are administered before or after surgery with the aim of eliminating occult micro-metastatic disease and improving disease-free and overall survival (1, 2). These treatments can reduce recurrences by as much as 50% (3–6). However, the administration of currently used cytotoxic agents often require venous access, are time-consuming, and can cause significant side effects. Clearly, alternative strategies that selectively target breast cancer cells and are less toxic are highly desirable.

The Na⁺/I⁻ symporter (NIS) is an intrinsic plasma membrane glycoprotein that mediates the active uptake of I⁻ in the thyroid and other tissues such as salivary glands, gastric mucosa, and lactating mammary gland (but not nonlactating). In these cells, NIS localizes along the basolateral surface of the plasma membrane (7–10). Using the Na⁺ gradient maintained by the Na⁺/K⁺ ATPase as its driving force, NIS couples the inward uphill translocation of I⁻ against its concentration gradient to the inward downhill translocation of Na⁺ in favor of its concentration gradient. In the thyroid, NIS-mediated I⁻ uptake is the key first step in the biosynthetic pathway of the I⁻-containing thyroid hormones triiodothyronine (T₃) and thyroxine (T₄). Hence, to mediate active I⁻ transport, NIS must be at the plasma membrane.

NIS is regulated differently in different tissues. For example, in the thyroid, NIS activity and expression are stimulated by thyroid-stimulating hormone (TSH), whereas in NIS-expressing extrathyroidal tissues, TSH has no effect on I⁻ transport. Physiologically, NIS is only expressed in the breast during lactation wherein I⁻ is actively transported into lactocytes and concentrated 60-fold in milk (7, 11–15). NIS function in postpartum lactocytes is critical in providing I⁻ for thyroid hormone biosynthesis in the infant. NIS activity in the mammary gland of lactating rodents starts at the end of gestation. After parturition, NIS activity is regulated by suckling. Functional NIS expression can be experimentally induced in nonlactating ovariectomized mice by the administration of the lactogenic hormones estrogen, prolactin, and oxytocin (7).

Taking advantage of the functional expression of NIS in thyroid cancer cells, ¹³¹I has been used for 60 years to successfully ablate thyroid cancer metastases (16–19). In principle, this

Received 1/13/04; revised 3/18/04; accepted 3/30/04.

Grant support: Susan G. Komen Breast Cancer Foundation Grant 99-3052.

The costs of publication of this article were defrayed in part by the payment of page charges. This article must therefore be hereby marked *advertisement* in accordance with 18 U.S.C. Section 1734 solely to indicate this fact.

Requests for reprints: Irene L. Wapnir, Department of Surgery, Stanford University School of Medicine, 300 Pasteur Drive, H-3625, Stanford, CA 94305-5655. E-mail: wapnir@stanford.edu.

same approach could be applied to women with breast cancer because NIS is also expressed in >70% of malignant breast cells (7, 8, 20–22). The association between I⁻ transport and NIS expression in mammary adenocarcinomas was first experimentally demonstrated in transgenic mice (*Ras* and *c-erbB-2*; Ref. 7). Because of these observations, we postulated that selective targeting of human breast cells with ¹³¹I might be feasible if NIS were functionally expressed. The concept was strengthened by the fact that thyroid and breast NIS are regulated by different mechanisms, which allows thyroid uptake to be blocked without affecting I⁻ transport in the breast. This can be accomplished by administering T₃, which inhibits TSH release from the hypophysis and thus leads to the concomitant down-regulation of thyroid NIS expression.

The uptake of radioiodide or ^{99m}TcO₄⁻ (technetium-pertechnetate, same charge and similar size as I⁻) by the lactating breast and secretion of these tracers in breast milk has been known for decades (12–15). Recently, Moon *et al.* (23) demonstrated ^{99m}TcO₄⁻ accumulation in 3 of 24 human primary breast carcinomas and found a positive correlation between uptake and higher levels of NIS mRNA. This finding is highly significant, but what still remained to be addressed was whether breast cancer metastases exhibited scintigraphically detectable NIS activity. The importance of the latter is the potential application of ¹³¹I therapy for the ablation of breast cancer metastases after removal of the primary tumor.

The untapped potential of NIS as a tool for the delivery of radioiodide in nonthyroidal tissues, particularly ¹³¹I, is underscored by a series of preclinical studies. Melanoma, prostate, breast, and glioma cancer cell lines accumulate I⁻ after NIS transfection and exhibit selective cell death when exposed to ¹³¹I (24–29). Tumor reduction or even disappearance has been shown in ¹³¹I-treated human prostate xenografts expressing NIS after viral gene transfer (27). These studies represent novel evidence that extrathyroidal tissues harboring functional NIS protein retain ¹³¹I for prolonged periods, resulting in tumor cell destruction in the absence of intracellular organification of I⁻ (28).

Before the present study, there have been no reports on the key issue of I⁻ uptake detected by scintigraphy in breast cancer metastases. This prospective study was undertaken to assess *in vivo* I⁻ accumulation in breast cancer metastases using scintigraphy and to estimate, by dosimetry, the feasibility of radioiodide ablation of metastases. NIS expression in archival tumor samples was correlated with scintigraphic findings. Importantly, thyroidal suppression was implemented and radiation dose to the thyroid and whole body calculated.

PATIENTS AND METHODS

Study Population. The Institutional Review Board (UMDNJ-Robert Wood Johnson Medical School) and the Administrative Panel on Human Subjects in Medical Research (Stanford University School of Medicine) reviewed and approved the study described herein. Women with metastatic breast cancer were asked to voluntarily participate in this trial. The intent and details of the proposed research, potential risks, and benefits were thoroughly explained, and written informed consent was obtained. Eligibility criteria included evidence of

metastasis at any distant site or locoregional recurrences consistent with a history of breast cancer. Documentation of disease on plain films, computed tomography of the chest, abdomen, or pelvis, bone scan, or magnetic resonance imaging was acceptable. Cytological or histological proof of metastasis was not required for entry into the study. Ongoing chemohormonal treatments were not interrupted.

Study Design. The protocol was initially designed to study NIS activity using ^{99m}TcO₄⁻ [a radioisotope also transported by NIS, with a shorter half-life (6 h) than ¹²³I and ¹³¹I and not organified in the thyroid] (30, 31). Each patient received 5–15 mCi of ^{99m}TcO₄⁻ and was imaged at 15, 30, 60 and 120 min. After 7 patients were imaged, we elected to switch to ¹²³I to better assess the retention time. Advantages of ¹²³I over ^{99m}TcO₄⁻ include a longer half-life and the possibility of calculating tissue/organ dosimetry (30).

All participants were asked to adhere to a low-I⁻ diet in preparation for the scan (32). Halfway through the study, T₃ (25 µg twice daily) was administered to every patient for 10–15 days to lower TSH below the normal range and evaluate selective suppression of thyroidal I⁻ uptake. Women taking thyroid hormone for preexisting thyroid disease remained on their medication.

Whole-body images in the anterior and posterior projections were obtained at 4 and 24 h after an oral dose of 1–2 mCi of ¹²³I. Three patients underwent baseline imaging at 1 h after tracer administration and before voiding to calibrate the injected dose. Thyroid gland uptake was calculated from the thyroid probe counts or by quantification of the whole-body scans in the latter group. Scans were interpreted blindly by nuclear medicine physicians without previous review of other radiological studies or details regarding sites of metastatic disease in these women.

If tracer was taken-up by tumoral tissues on the first scan, patients were invited to undergo a second whole-body dosimetry scan using 2 mCi of ¹³¹I. To maximally suppress thyroidal uptake and simulate treatment conditions, methimazole (MMI; 20 mg) was added to the T₃ regimen, beginning 10 days before the scan and continuing over 5 days after the ingestion of the tracer. Tumor, thyroid, and whole-body radiation doses were estimated to determine whether tumor ablation could be achieved.

Scintigraphy. A whole-body scanner was used to image whole-body distribution. For ¹²³I, a low-energy, high-resolution collimator with a scanning speed of 10 cm/min over 180–200 cm was used. The window was set at 159 keV ±15%. In the case of ¹³¹I, a high-energy collimator (up to 450 keV) was used with a scanning speed of 12 cm/min and a window setting of 364 keV ±15%. Counts were obtained from the regions of interest over the whole body or the thyroid in anterior and posterior images. Geometric averages for anterior and posterior counts were used. The counts were calibrated to the counts at time *t* < 60 min before any voiding.

Immunohistochemistry. NIS expression was evaluated by immunohistochemical methods on archival tissue specimens. Metastatic tissues were analyzed whenever possible. In many instances, primary breast tumors were the only available samples. In brief, 5-µm sections were deparaffinated in xylene and rehydrated through graded alcohols. Then antigen retrieval was performed at 95°C for 45 min with 10% citrate buffer solution

obtained from DAKO (Carpinteria, CA). After cooling slides, endogenous peroxidase was quenched with 3% peroxide. Slides were sequentially incubated with avidin, biotin, and protein block from DAKO. An anti-NIS polyclonal antibody (Ab) directed against the last 16 amino acids of the COOH-terminal peptide of human NIS (residues 632–643, GHDGGRDQ-ETNL) was affinity purified before using (15, 16). Slides were incubated for 15 min with Ab diluted in serum-free protein. The specificity of the Ab was corroborated by peptide competition, resulting in the absence of immunoreactivity. Human salivary gland sections were included in every experiment as positive controls; the same were also tested with secondary Ab in the absence of primary Ab as negative control. The remainder of the immunoperoxidase procedure was carried out according to the supplier's instructions provided in the Catalyzed Signal Amplification kit from DAKO.

Slides were analyzed by light microscopy. NIS immuno-

reactivity was characterized as negative if $\leq 20\%$ of the cells showed NIS immunoreactivity. Positivity was graded simply as weakly positive or strongly positive, respectively, if $\geq 20\%$ of cells demonstrated brown staining associated with the immunoperoxidase reaction. The presence of plasma membrane immunoreactivity was noted. In the case of discordant results between the index tumor and the metastasis, the latter was used in the final consideration.

RESULTS

Twenty-seven patients with metastatic breast cancer underwent $^{99m}\text{TcO}_4^-$ or ^{123}I scans. These results were correlated with immunohistochemical findings in 23 cases predicated on the availability of evaluable tumor blocks (Table 1). The mean age of women on this study was 50.4 years (range, 38–76 years). Eighteen patients had metastasis involving multiple organs or

Table 1 Correlation between I^- scintigraphy and NIS expression

	T_3^a	T_4	TSH $\mu\text{IU/ml}$	Scintiscan	Thyroid uptake ^{123}I @ 24 h ^b	Thyroid uptake ^{131}I @ 24 h ^b	Metastasis	Tissues	NIS expression	Estrogen receptor in index tumor or metastasis	Ongoing therapy
							% Uptake of ingested dose	(Index tumor or metastasis)			
1				$^{99m}\text{TcO}_4$			—	M (soft tissue)	Neg	—	+
2 ^c				$^{99m}\text{TcO}_4$			—	M (soft tissue)	Pos	—	+
3				$^{99m}\text{TcO}_4$			—	I	Neg	+	+
4				$^{99m}\text{TcO}_4$			~1%	M (soft tissue)	Pos	—	—
5				$^{99m}\text{TcO}_4$			—	I	Neg	+	+
6				$^{99m}\text{TcO}_4$			—	I	Neg	—	+
7				$^{99m}\text{TcO}_4$			—	I	Neg	—	+
8				^{123}I			—	I	Neg	+	+
9				^{123}I			—	M (soft tissue)	Neg	+	+
10		X ^d	0.3	^{123}I	0%		—	I	Pos	+	+
11				^{123}I	20.3%		—	I	Neg	+	+
12				^{123}I	48%		—	NA	NA	+	+
13		X	4.2	^{123}I	11%		—	NA	NA	+	+
14	X		0.088	^{123}I	1.4%	2.5% (4 h) ^e	2.9%	I	Pos	—	+
	X+		0.031	^{131}I		0.22% (24 h)	—	M (lung)	Pos		
	MMI					0.048% (48 h)	—				
						0.035% (72 h)	—				
15	X		0.036	^{123}I	0.9%		—	M (bone)	Neg	—	+
16		X	2.1	^{123}I	Minimal		—	M (lymph node)	Neg	—	—
17	X		0.572	^{123}I	3.8%		—	I	Pos	—	+
18	X		0.019	^{123}I	2.0%		—	NA	NA	+	+
19	X		0.014	^{123}I	1.4%		—	NA	NA	+	+
20	X		0.007 ^f	^{123}I	4.6%		—	I	Neg	+	+
21	X		Not done	^{123}I	2.0%		—	I	Neg	—	+
							—	M (soft tissue)	Neg	—	—
22	X		0.018	^{123}I	1.7%		—	I	Pos	—	+
23	X		0.135	^{123}I	Trace		—	I	Pos	—	—
24	X		0.33	^{123}I	2.7%		—	I (axillary lymph)	Pos	—	+
25	X		0.054	^{123}I	2.8%		—	M (soft tissue)	Neg	—	+
26	X		0.00	^{123}I	1.99%		—	I (recurrent breast)	Neg	—	+
27	X		0.079	^{123}I	1.26%		—	I (\rightarrow metastasis)	Neg	+	+
							—	Contralateral primary	Pos	—	+

Note: Bold designates the NIS-positive cases.

^a T_3 , triiodothyronine; T_4 , thyroxine; TSH, thyroid-stimulating hormone; NIS, Na^+/I^- symporter; M, metastasis; Neg, negative; Pos, positive; I, index or primary breast cancer; NA, not available; MMI, methimazole.

^b Handheld probe.

^c Bold designates the NIS-positive cases.

^d Primary hypothyroidism.

^e Scintigraphic calculation.

^f Performed 1 week before scan.

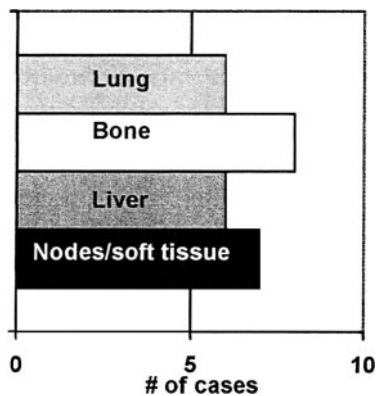


Fig. 1 Sites of breast cancer metastasis. Cases grouped according to predominant site of metastatic disease. Eighteen of these patients had additional involvement of other organs.

tissues. Fig. 1 shows the distribution of cases according to the tissue or organ predominantly involved with metastatic disease: soft tissue and/or lymph node in 7 cases; liver in 6 cases; lung in 6 cases; and bone in 8 cases. Four patients in this series had metachronous bilateral breast cancer, one of which was newly discovered and present at the time of the scintiscan. Interestingly, 3 patients had estrogen receptor (ER)-positive breast cancers with metachronous contralateral ER-negative tumors. Fourteen cases were considered ER negative based on the hormone status of the metastasis or, if unavailable, relying on the results of the primary lesion. All but 2 patients studied were receiving concomitant hormonal therapy, chemotherapy, trastuzumab (Herceptin), or a combination of these. Two patients were deemed eligible for the ^{131}I dosimetry scan after the initial $^{99\text{m}}\text{TcO}_4^-$ or ^{123}I scans, but only one completed the study.

Scintigraphy. The first 7 patients were evaluated scintigraphically with $^{99\text{m}}\text{TcO}_4^-$. None of these patients was medicated with thyroid hormones. Patient A (no. 4 in Table 1) showed localization of the tracer in a histologically proven ER-negative, unresectable, ulcerated, axillary recurrence (Fig. 2A). NIS immunoreactivity was present in $>30\%$ of metastatic tumor cells. Both patient and treating physician declined participation in the ^{131}I dosimetry study.

The remaining 20 patients were imaged with ^{123}I . Included among these patients were 3 who were receiving systemic therapy and who turned out to have no evidence of metastatic disease on follow-up imaging studies, suggesting that perhaps at the time of their scans little disease, if any, was present. Another patient in this group had longstanding stable bone disease and a new contralateral primary breast tumor.

Patient B (no. 14 in Table 1) had a history of an ER-negative, Her2-neu-positive right lung metastasis with involved regional nodes. On the ^{123}I scan, focal tracer localization was noted in the vicinity of the right pulmonary hilum (Fig. 2B) in conjunction with low thyroid accumulation of 1.4% on handheld probe (on T_3 for thyroid suppression; 0.088 $\mu\text{IU/ml}$ TSH). Imaging studies performed several months before did not show recurrent lung disease in this region. Accumulation was visualized at 4 h on the posterior view only and was not identified on the 24-h scan. Contrastingly, thyroid uptake was noted on the

anterior projection only. The detection of uptake on one projection but not the other is consistent with the attenuating effects of body mass and distance from the source. However, in the succeeding months, an endobronchial metastasis occupying the right bronchus was diagnosed and a chest computed tomography scan (Fig. 2C) demonstrated a recurrent hilar mass with regional lymphadenopathy. These findings suggest that tracer uptake could coincide with the tumor or paratracheobronchial lymph nodes. So, 8 months later, a dosimetry scan was performed using 2 mCi of ^{131}I . MMI (which blocks I^- organification) was administered in addition to T_3 , resulting in a prescan TSH of 0.031 $\mu\text{IU/ml}$. Again, I^- uptake was noted in the same area corresponding to the lung metastasis (Fig. 2B). Accumulation was calculated as 2.9% of the administered dose at 4 h, whereas I^- uptake in the suppressed thyroid gland was 2.49%. As on the ^{123}I scan, the signal disappeared by 24 h. The I^- uptake observed by scintigraphy in the pulmonary or nodal metastasis of this patient and its correlation to NIS expression in the metastatic lung tumor is a key finding of this study. No such uptake in a site of breast cancer metastasis has ever been reported before.

Thyroidal Accumulation. Three women were on thyroid hormone (T_4) medication for preexisting hypothyroidism (case nos. 10, 13, and 16 in Table 1). Eleven patients were scanned without the use of any thyroid hormone preparation. One woman in this subgroup was found unexpectedly to be hyperthyroid [uptake of 48% at 24 h (no. 12, Table 1)]. Once the protocol was modified, 13 subjects were premedicated with T_3 in preparation for the study. Their prescan TSH levels ranged from undetectable to 0.572 (normal range, 0.4–4.0 $\mu\text{IU/ml}$). $^{123}\text{I}^-$ uptakes of 0.9–4.6% were observed in this group (Table 1 and Fig. 3). For the patients whose serum TSH was subnormal (<0.4 $\mu\text{IU/ml}$) before scanning, thyroid uptake was correspondingly $\leq 2.8\%$ of the administered dose. Higher uptakes were noted in 2 patients who, unbeknownst to the physicians, failed to take T_3 on the day of the scan, one of which also had a TSH value in the normal range (Fig. 3). Even so, $^{123}\text{I}^-$ thyroid accumulation was markedly suppressed in medication-compliant patients (0.9–2.8%) compared with two unsuppressed patients in this series (20–22%) or to the ranges reported in the literature (8–35%) (32). No untoward effects were noted in any of the patients upon either receiving or stopping this treatment.

Dosimetric Calculations. Imaging was performed with $^{123}\text{I}^-$ on 3 patients at 1, 4, and 24 h, allowing for the calculation of dosimetry and estimation of cumulative radiation dose for ^{131}I . All 3 patients were medicated with T_3 therapy without methimazole. Whole-body and thyroid cumulative activity were computed and expressed as mCi.hr or % ingested dose of either $^{123}\text{I}^-$ or ^{131}I after correction for physical decay. The limitation of dose estimates rests on the extrapolations made after the last measured point. Herein, the effective half-life is assumed to be equal to the physical half-life of ^{131}I under medical internal radiation dose 3 assumptions after the 24-h measurement (33). Therefore, under these conditions, if 100 mCi of ^{131}I were administered, the radiation dose to the thyroids of these 3 patients would be between 13,000 and 27,000 cGy and between 55 and 115 cGy to the whole body. For a metastasis, the estimate is more speculative because of the uncertainties of tumor size and weight. If a tumor were the size of the thyroid

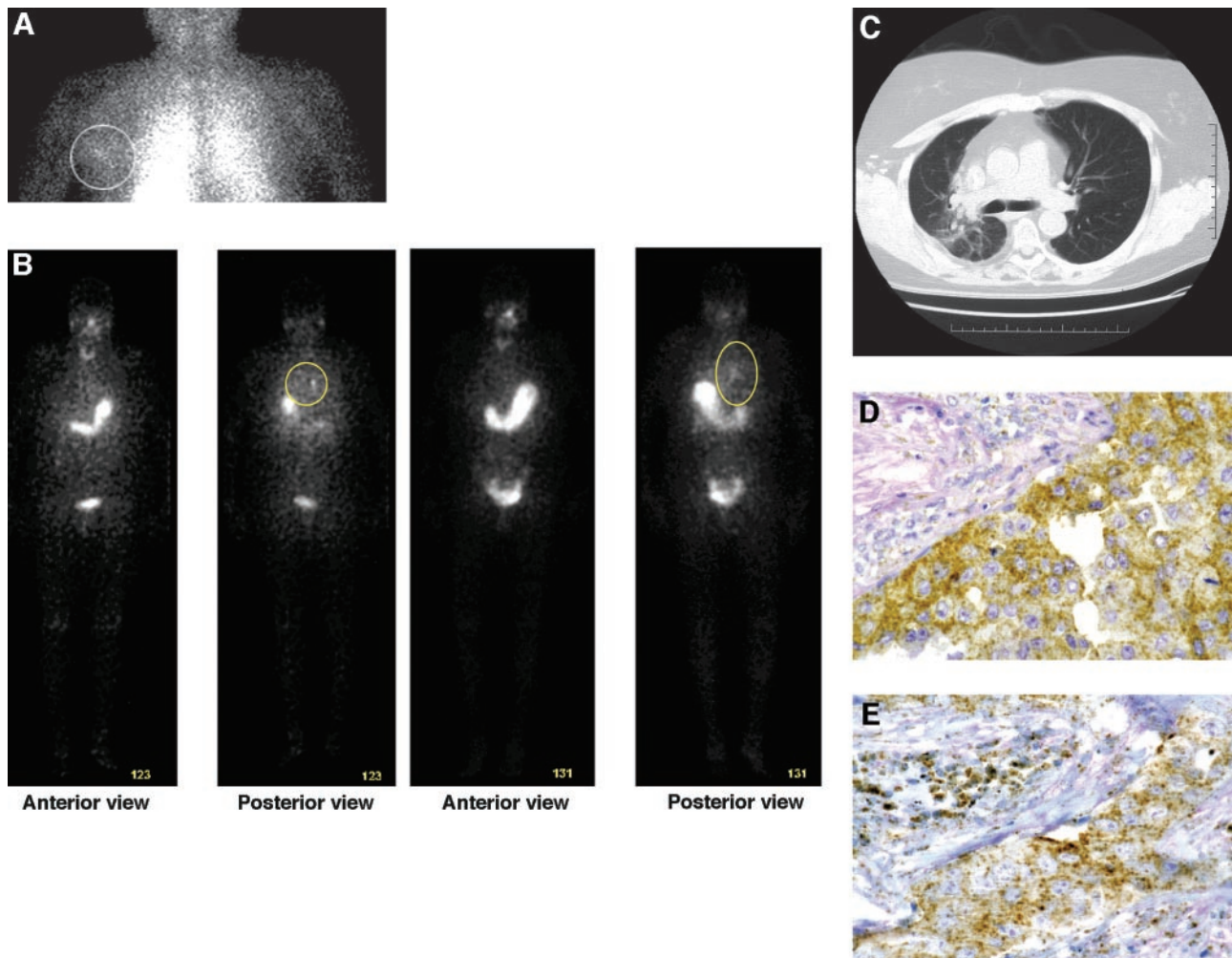


Fig. 2 ^{99m}Tc -pertechnetate, ^{123}I , and ^{131}I uptake scans in Na^+/I^- symporter (NIS)-positive metastatic breast cancer. **A**, ^{99m}Tc -pertechnetate scan showing uptake at 30 min in axillary metastasis indicated by *circle*. **B**, ^{123}I scintiscan performed after a 10-day course of T_3 thyroid-suppressive treatment (TSH; 0.088 $\mu\text{IU}/\text{ml}$). Anterior and posterior projection is shown here taken at 4 h. Tracer is noted in the stomach, small bowel, and bladder. Accumulation is seen in the perihilar region of the right lung (*yellow circle*) at the site of metastasis on the posterior view only. Similar images represent ^{131}I scans obtained months later. **C**, computed tomography scan of chest performed weeks before ^{131}I scan shows an irregular mass in the region of the right hilum (*black arrow*) corresponding to the bronchoscopy proven breast cancer metastasis. **D**, primary invasive ductal carcinoma of the breast showing 3+ immunoreactivity to anti-NIS antibody. Because of the strong immunoreactivity, presence or absence of plasma membrane immunopositivity cannot be discerned, original magnification, $\times 60$. **E**, focally intense NIS immunoreactivity in malignant breast cells metastatic to lung, original magnification, $\times 30$.

gland (~ 20 g) and the ^{131}I kinetics comparable with the T_3 -treated-only thyroid gland, then the dose would be similar. A corresponding increase would occur for a tumor that is 5 or 10 times smaller but has similar uptake and kinetics.

In one case (patient B, no. 14; Table 1), imaging was performed with ^{131}I at 4, 25, 48, 72, and 96 h, and the cumulative activity in the thyroid and whole body were measured. This subject received MMI (to block I^- organification) in addition to T_3 to further decrease accumulation of I^- and improve protection of the thyroid during ^{131}I administration. Thyroid gland uptake was calculated as 2.49% (4 h), 0.52% (24 h), 0.12% (48 h), and 0.079% (72 h). Handheld thyroid probe measurements were lower with 0.22% at 24 h, 0.048% at 48 h, and 0.035% at 72 h. Again after 72 h, effective half-life was

assumed to be equal to physical half-life. Using this approach, we estimated the cumulative radiation dose to the whole body and thyroid for 100 mCi of ^{131}I as 333 and 15 cGy, respectively. Now, if patient B's lung metastasis [~ 2 g based on computed tomography measurements (2.1×1.7 cm)], which accumulated 2.9% ingested dose of the administered ^{131}I dose at 4 h, exhibited the same dynamics as her T_3 /MMI-suppressed thyroid gland (~ 20 g), then 10 times the radiation dose could be concentrated or ~ 3000 cGy. On the other hand, if the dynamics of the tumor metastasis approximated those achieved in the thyroid with T_3 suppression only, then the radiation dose to the metastasis would be considerably higher.

In conclusion, these calculations suggest that the use of ^{131}I doses with potential therapeutic effectiveness in human breast

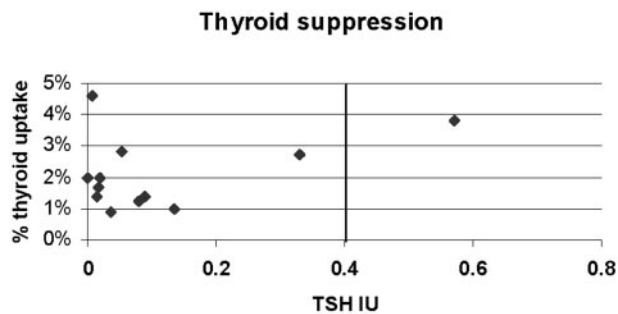


Fig. 3 ^{123}I thyroid uptake as a function of thyroid-stimulating hormone (TSH) in thyroid-suppressed patients. Twelve patients were treated with T_3 before ^{123}I scan and had TSH measured before scintigraphic evaluation. TSH was subnormal range ($<0.4 \mu\text{IU/ml}$) in 11 cases, associated with thyroid uptakes of $\leq 2.8\%$. One other patient had a TSH level of $0.007 \mu\text{IU/ml}$ recorded 4 days before the scan and then exhibited an uptake of 4.6% as a result of skipping prescan doses.

cancer metastases is feasible and may thus represent a novel targeted treatment strategy that may not only be better but also safer and less expensive than currently used approaches.

NIS Protein Expression. Archival specimens were obtained for 23 of the 27 patients participating in the study. Metastatic tissue was evaluable in 9 patients (39%), and in 6 cases, both the primary tumors and the metastasis were evaluated. The samples available in the remaining 14 cases represented primary breast cancers and/or the corresponding involved axillary nodes. NIS expression was positive in 8 (34.8%) cases and negative in 15 (65.3%) cases, including 2 in which the primary cancers were weakly positive and the metastases were deemed negative. As stated earlier, whenever metastatic samples were available, the immunohistochemical analysis of these was used to define the case as positive or negative rather than the index tumor. Three of 9 metastatic samples and 5 of the 14 (35.7%) primary or index archival samples were immunopositive. Overall, only 8 cases (34.8%) were ER-positive tumors, and 7 (87.5%) of the 8 NIS-positive cases were characterized as ER-negative tumors.

NIS immunoreactivity was observed in two patterns: one, as areas of NIS-positive tumor cells within a tissue section (Fig. 4A, B, and E), or two, as scattered immunopositive tumor cells interspersed among NIS-negative tumor cells (Fig. 4C). Thus, uptake was identified in 2 of 8 cases (25%) exhibiting NIS expression by our definitions. If we consider only those cases where metastatic samples were assessed, then it is notable that radioisotope uptake was observed in 2 of 3 (66%) NIS-positive cases. Intense NIS expression is shown in Fig. 4A, corresponding to the tissue from the $^{99\text{m}}\text{TcO}_4^-$ -accumulating metastasis of patient A (no. 4; Table 1, Fig. 2A). Strong immunoreactivity was detected too in both the primary tumor and the recurrent lung metastasis of patient B depicted in Fig. 2. NIS expression was observed in cases with axillary nodal metastasis (Fig. 4, C and D) whose scans did not demonstrate I^- uptake. These tumor-containing tissues were removed 2 and 8 years earlier before there was evidence of metastatic disease in these patients. In another instance (patient no. 27), no scintigraphic accumulation was noted in a new contralateral breast primary tumor, which

demonstrated NIS immunopositivity. Disease progression or therapeutic interventions may affect NIS functional expression and explain the absence of I^- accumulation on scintiscans.

DISCUSSION

In this study, we demonstrate that some NIS-expressing human breast cancers accumulate I^- at sites of known metastatic disease. To our knowledge, this is the first prospective clinical trial aimed at evaluating the I^- accumulating capacity of breast cancer metastases and the first study to demonstrate *in vivo* I^- uptake in breast cancer metastasis on scintigraphy. In the current study 8 of 23 (34.8%) of the evaluable samples expressed NIS significantly. I^- transport in metastases was demonstrated in 2 of 8 (25%) women with NIS-expressing cancers. The prevalence of NIS expression in this cohort of patients with metastatic disease was lower than reported by us in a larger sample of cases (7, 8). In that survey, $>70\%$ of 228 invasive breast carcinomas (91 conventional sections and 137 microarray tissue cores) exhibited NIS immunopositivity. Fresh-frozen or archival specimens of breast cancer metastasis are more difficult to obtain because fine-needle aspiration cytology is increasingly used to confirm the presence of distant disease. It is important to point out that NIS expression can readily be assessed in cell aspirates so that the near-routine determination of NIS expression in breast cancer metastases could be implemented with relative ease in the near future (34). Presently, the correlation of I^- transport to NIS expression is mostly done on sections of index breast tumors or axillary node metastasis because metastatic tissue is not readily available.

It is possible that the proportion of cases demonstrating I^- transport among NIS-expressing tumors would have been higher if the tested tissue samples had been harvested contemporaneously. In fact, most archival tissues studied were retrieved at earlier time points, and therefore, residual tumor cells may have lost the ability to express NIS in the interim. It is also plausible that either through disease progression or via the effects of interval or concurrent treatments (24 subjects), NIS protein expression and/or function could have been altered. Two of our cases illustrate this phenomenon, wherein weak immunoreactivity was observed in the primary tumor but lost in the metastasis. NIS was detected in 5 cases in which no scintigraphic accumulation was noted. However, in all instances, 1–8 years elapsed between the time of tissue removal and the *in vivo* scan. In the interim, adjuvant therapies and subsequent treatments for metastatic disease may have eliminated these NIS-expressing malignant cells. Alternatively, relatively little NIS protein may be present in the plasma membrane despite overall microscopic appearance of strong immunoreactivity, accounting for the absence of tracer accumulation on scintigraphy. In the treatment of thyroid cancer metastases, thyroid hormone replacement therapy is withdrawn or recombinant TSH is administered to augment the I^- uptake capacity of these cells (32, 35). It has been shown by Reidel *et al.* (36) that plasma membrane targeting of NIS in rat thyroid cells is regulated by TSH. No such mechanism has been identified in breast tissue, underscoring the need to understand the factors influencing plasma membrane targeting and NIS activity in breast cells.

Nearly all NIS-expressing tumors were ER negative, sug-

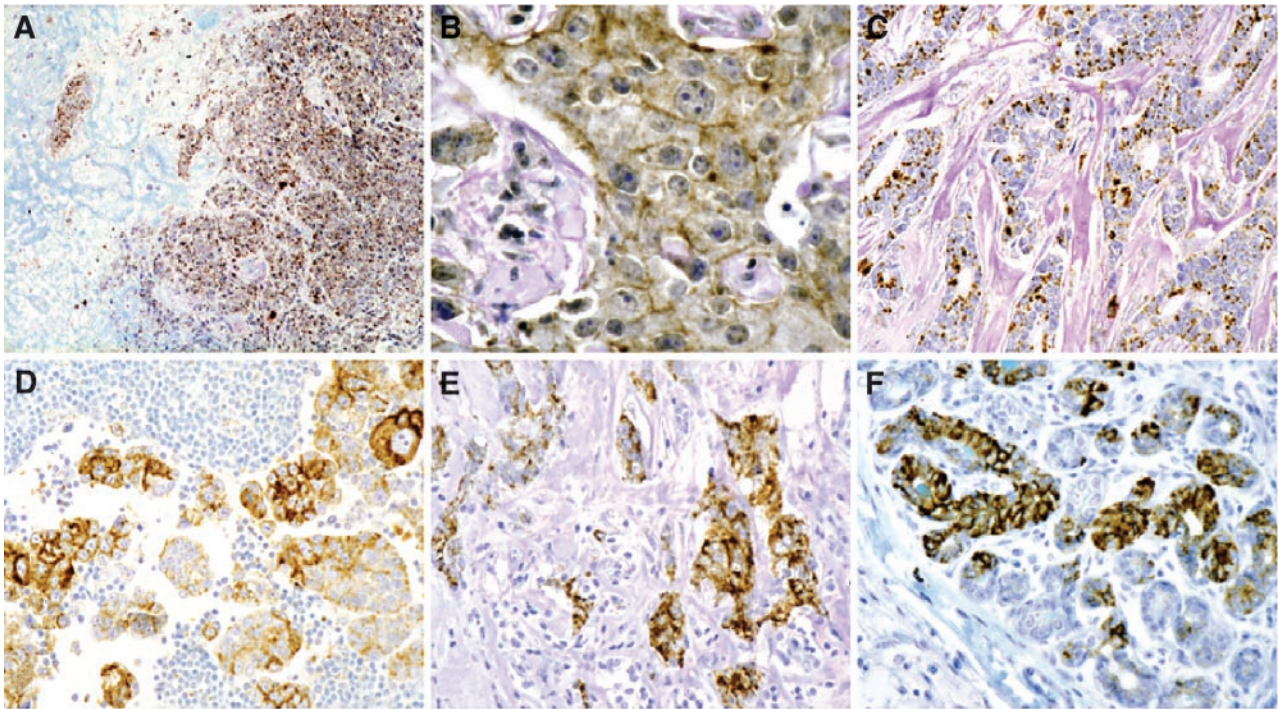


Fig. 4 Immunohistochemical findings in breast cancer metastasis. **A**, immunoreactivity in unresectable axillary metastasis, $\times 20$. **B**, intracellular and distinct plasma membrane immunoreactivity in primary breast, $\times 80$. **C** and **D**, Na^+/I^- symporter (NIS)-positive breast cancer cells in axillary lymph node metastasis, $\times 40$. **E**, contralateral second primary showing strong NIS immunoreactivity in patient with negative metastasis from index tumor, $\times 40$. **F**, strong immunopositivity in normal breast lobules of NIS-negative breast cancer, $\times 40$.

gesting that up-regulation of NIS in malignant cells may be an estrogen-independent event. This phenomenon was previously noted in animal models whereby transgenic mice carrying spontaneous estrogen-independent mammary carcinomas expressed NIS and accumulated I^- (7). This contrasts with the physiological hormonal effects known to be operant during gestation, suckling, and lactation and associated with NIS expression (7, 11).

In thyroid cancer, postthyroidectomy ^{131}I -ablative treatments have decreased recurrences from 30 to 8% (32). The application of ^{131}I radiotherapy to the treatment of breast cancer would be derived from the thyroid experience and strengthened by similarities in the pattern of NIS immunoreactivity observed in both cancers (8, 37, 38). The feasibility of ^{131}I radioablation depends on the biological half-life of the isotope in the target breast cancer cells, the dose of radioactivity attained in these tumors, and the ability to block accumulation in the thyroid gland. NIS protein is detectable in tissues from some patients who failed to demonstrate accumulation of I^- on scintigraphic studies. It is likely that transport activity below a certain threshold is too low for scintigraphic detection. Alternatively, NIS in these tissues may not be at the cell surface, the only cellular location where NIS mediates I^- transport. The factors that up-regulate functional expression of NIS in breast carcinoma cells are just being identified. Recently, induction of functional NIS expression upon addition of all-*trans*- and 9-*cis*-retinoic acid to MCF-7 cells or administration to immunosuppressed mice carrying MCF-7 xenografts was reported (39–41). Once all regu-

latory factors are known, breast cancers with low NIS expression could be stimulated to increase NIS biosynthesis and/or activity. Indeed, stimulation of I^- uptake in postthyroidectomy thyroid cancer patients is routinely achieved by administration of TSH or withdrawing thyroid hormone medications. The success of this approach could reside in the selection of an appropriate subset of breast cancer patients, those with limited regional disease or clinically occult metastases, as is often done in thyroid cancer patients (35, 42, 43).

A substantial advantage of ^{131}I therapy is that it is well tolerated, given as a single oral dose, and is inexpensive. Side effects are usually minor and limited, mostly nausea/vomiting, transient pain, and swelling of the salivary glands, gastritis, and cystitis. Other far less common but more serious toxicities such as leukemia or myelodysplasia can occur in $<0.5\%$ cases, especially if whole bod-/blood radiation doses exceed 2 Gy (32). Overall, selective targeting of cancer cells with radioactive iodide represents less toxicity to organs not involved with I^- or its excretion. Several preclinical studies have demonstrated the ablative effects of ^{131}I in tumor xenografts in the absence of organification (25–28). Ultimately, additional studies exploring the *in vivo* dynamics of I^- in NIS-expressing cancers and the underlying molecular mechanisms of radioiodide in cancer cells will determine the true potential success of targeting nonthyroidal cancers with ^{131}I in tissues not known to organify I^- . Alternatively, NIS may be used to transport other radioisotopes such as the β -emitter ^{188}Re rhenium, which could potentially be more effective than ^{131}I because of higher radiation (44, 45). How-

ever, the only clinical experience with this radioisotope is limited to its use for endovascular brachytherapy or treatment of osseous metastasis (46, 47).

Radioablation of nonthyroidal cancers such as breast would be hampered in theory by the thyroid's exquisite capability of accumulating and organifying I. If left intact, the thyroid would be exposed to excessive radiation, regional inflammation, and hypothyroidism. A pertinent example of ^{131}I -induced thyroid toxicity is the experience and outcomes of patients treated with ^{131}I -tagged monoclonal Abs for lymphoma given that ^{131}I is cleaved from the ^{131}I -Abs in the bloodstream. This nontherapeutic-free ^{131}I is concentrated in the thyroid, causing hypothyroidism (48–50). Despite pre- and posttreatment use of Lugol's solution (concentrated KI) aimed at saturating iodide stores and decreasing uptake in I-transporting organs, hypothyroidism occurs in up to 64% of patients within the first year of treatment (50, 51). The T_3 regime we used in this study to minimize thyroid ^{131}I uptake may prove more effective than the standard Lugol therapy, considering that the latter not only decreases thyroidal ^{131}I uptake by competition of cold I with ^{131}I , but also causes more ^{131}I to remain in the system longer because cold I competes with ^{131}I in the kidneys and thus slows the excretion rate of ^{131}I .

The protocol we developed in the course of this trial was directed at maximally reducing thyroidal accumulation without affecting extrathyroidal I transport. TSH regulates I uptake in the thyroid gland exclusively, thus the administration of thyroid hormones can be used to interfere with this mechanism, resulting in a lowering of TSH and the consequent down-regulation of thyroid NIS expression (52). We show in our study that even with moderate doses of T_3 taken twice daily for 10–15 days, thyroidal I uptake decreased to <3% at 24 h. This represents approximately a 75% reduction in thyroid I accumulation. MMI provided additional protection, reducing accumulation by 90% (0.22%) at 24 h by impeding the intracellular organification of I as was shown on the ^{131}I dosimetry study. A similar approach to thyroid protection has recently been reported by van Santen *et al.* (53) in pediatric patients being treated with ^{131}I metaiodobenzylguanidine for neuroblastoma. In that study, a combination of KI/ T_4 /MMI was successfully used to preserve thyroid function after treatment with the radioiodinated pharmaceutical. On the basis of the above-mentioned I renal secretion, those patients might benefit even more from a T_3 /MMI combination treatment. We estimate that combination therapy with T_3 and methimazole would result in a radiation dose for the thyroid gland of ~300 cGy following a therapeutic dose of 100 mCi of ^{131}I . At these doses, radiation thyroiditis or hypothyroidism are unlikely. More frequent T_3 dosing (three times/day) may reduce even further the amount of radioiodide entering the thyroid gland.

In summary, we have demonstrated that NIS-mediated I uptake is scintigraphically detectable *in vivo* in breast cancer metastases. We conclude that ^{131}I radioablation of at least some breast cancer metastases is potentially feasible with minimal radiation to the thyroid, holding out the near-term prospect of a novel and possibly better therapeutic approach for this disease.

ACKNOWLEDGMENTS

We thank Drs. I. Ross McDougall, Beatriz Lega, Gayle Holtzman, Robert Carlson, and Louis Amorosa for their clinical assistance and support of this research effort. We also thank Angelina Owens, Marcia Anderson, and Caroline Tudor for their assistance.

REFERENCES

- Harris JR, Lippman M, Morrow M, Osborne CK. Diseases of the breast. Philadelphia: Lippincott, Williams & Wilkins; 2000.
- Carlson RW, Anderson BO, Bensinger W, et al. The NCCN Breast Cancer Clinical Practice Guidelines in Oncology. J Natl Comprehensive Cancer Netw 2003;1:148–88.
- Fisher B, Dignam J, Wolmark N, et al. Tamoxifen and chemotherapy for lymph node negative disease, estrogen receptor-positive breast cancer. J Natl Cancer Inst (Bethesda) 1997;89:1673–82.
- Early Breast Cancer Trialists' Collaborative Group. Tamoxifen for early breast cancer: an overview of randomised trials. Lancet 1998;351:1451–67.
- Early Breast Cancer Trialists' Collaborative Group. Polychemotherapy for early breast cancer: an overview of randomised trials. Lancet 1998;352:930–42.
- Citron M, Berry D, Cirincione C, et al. Randomized trial of dose-dense *versus* conventionally scheduled and sequential *versus* concurrent combination chemotherapy as postoperative adjuvant treatment of node-positive primary breast cancer: first report of intergroup trial C9741/ Cancer and Leukemia Group B trial 9741. J Clin Oncol 2003;21:1431–9.
- Tazebay U, Wapnir IL, Levy O, et al. The mammary gland iodide transporter is expressed during lactation and in breast cancer. Nat Med 2000;6(8):871–8.
- Wapnir IL, van de Rijn M, Nowels K, et al. Immunohistochemical profile of the sodium/iodide symporter in thyroid, breast, and other carcinomas using high density tissue microarrays and conventional sections. J Clin Endocrinol Metab 2003;88:1880–8.
- Spitzweg C, Joba W, Schriever K, Goellner JR, Morris JC, Heufelder AE. Analysis of human sodium iodide symporter immunoreactivity in human exocrine glands. J Clin Endocrinol Metab 1999;84:4178–84.
- Vayre L, Sabourin JC, Caillou B, Ducreaux M, Schlumberger M, Bidard JM. Immunohistochemical analysis of Na^+/I^- symporter distribution in human extrathyroidal tissues. Eur J Endocrinol 1999;141:382–6.
- Cho J, Leveille R, Kao R, et al. Hormonal regulation of radioiodide uptake activity and Na^+/I^- symporter expression in mammary glands. J Clin Endocrinol Metab 2000;85(8):2936–43.
- Numberger CE, Lipscomb A. Transmission of radioiodine (I^{131}) to infants through human maternal milk. J Am Med Assoc 1952;150:1398–400.
- Honour AJ, Myant NB, Rowlands EN. Secretion of radioiodine in digestive juices and milk in man. Clin Sci 1952;11:447–62.
- Mountford PJ, Coakley AJ, Fleet IR, Hamon M, Heap RB. Transfer of radioiodide to milk and its inhibition. Nature (Lond.) 1986;322:600.
- Robinson PS, Barker P, Campbell A, Henson P, Surveyor I, Young PR. Iodine-131 in breast milk following therapy for thyroid carcinoma. J Nucl Med 1994;35:1797–801.
- Keston A, Ball R, Kneeland Frantz V, Palmer W. Storage of radioactive iodine in a metastasis from thyroid carcinoma. Science (Wash. DC) 1942;95:362–3.
- MacArthur JW, Cope O. The functional capacity of thyroid tumors as judged by radioactive iodine uptake. J Clin Invest 1946;25:929.
- Seidlin S, Rossman I, Oshry E, Siegel E. Radioiodine therapy of metastases from carcinoma of the thyroid: a six year progress report. J Clin Endocrinol 1949;9:1122–37.
- Dobyns B, Maloof F. The study and treatment of 119 cases of carcinoma of the thyroid with radioactive iodine. J Clin Endocrinol 1951;11:1323–60.

20. Dai G, Levy O, Carrasco N. Cloning and characterization of the thyroid iodide transporter. *Nature (Lond.)* 1996;379:458–60.
21. Smanik P, Liu Q, Furminger T, et al. Cloning of the human sodium iodide symporter. *BBRC* 1996;226:339–45.
22. Levy O, Dai G, Riedel C, et al. Characterization of the thyroid Na⁺/I⁻ symporter with an anti-COOH terminus antibody. *Proc Natl Acad Sci USA* 1997;94:5568–73.
23. Moon DH, Lee SJ, Park KY, et al. Correlation between 99m-Tc-pertechnetate uptakes and expressions of human sodium iodide symporter gene in breast tumors tissues. *Nucl Med Biol* 2001;28:829–34.
24. Mandell RB, Mandell LZ, Link C. Radioisotope concentrator gene therapy using the sodium iodide symporter gene. *Cancer Res* 1999;59:661–8.
25. Spitzweg C, O'Connor M, Bergert E, et al. Treatment of prostate cancer by radioiodine therapy after tissue-specific expression of the sodium iodide symporter. *Cancer Res* 2000;60:6526–30.
26. Boland A, Ricard M, Opolon P, et al. Adenovirus-mediated transfer of the thyroid sodium/iodide symporter gene into tumors for a targeted radiotherapy. *Cancer Res* 2000;60:3484–92.
27. Spitzweg C, Dietz AB, O'Connor MK, et al. *In vivo* sodium iodide symporter gene therapy of prostate cancer. *Gene Ther* 2001;8:1524–31.
28. Cho JY, Shen DH, Yang W, et al. *In vivo* imaging and radioiodine therapy following sodium iodide symporter gene transfer in animal model of intracerebral gliomas. *Gene Ther* 2002;9(17):1139–45.
29. Schipper ML, Weber A, Behe M, et al. Radioiodide treatment after sodium iodide symporter gene transfer is a highly effective therapy in neuroendocrine tumor cells. *Cancer Res* 2003;63:1333–8.
30. Links JM. Radiation physics. In: Braverman LE, Utiger RD, editors. *Werner and Ingbar's the thyroid: a fundamental and clinical text*. Philadelphia: J. B. Lippincott; 2000. p. 333–44.
31. McDougall R, Cavalieri R. *In vivo* radionuclide tests and imaging. In: Braverman LE, Utiger RD, editors. *Werner and Ingbar's the thyroid: a fundamental and clinical text*. Philadelphia: J. B. Lippincott; 2000. p. 355–75.
32. Mazzaferri E. Radioiodine and other treatments and outcomes. In: Braverman LE, Utiger RD, editors. *Werner and Ingbar's the thyroid: a fundamental and clinical text*. Philadelphia: J. B. Lippincott; 2000. p. 904–929.
33. Ellett WH, Reddy AR. Absorbed fractions for photon dosimetry. *J Nuc Med* 1968;9:(Suppl. 1):27–39.
34. Dohan O, De La Vieja A, Paroder V, et al. The sodium/iodide symporter (NIS): characterization, regulation and medical significance. *Endocr Rev* 2003;24:48–77.
35. Schlumberger M, Challeton C, De Vathaire F, Parmentier C. Treatment of distant metastases of differentiated thyroid carcinoma. *J Endocrinol Investig* 1995;18:170–2.
36. Reidel C, Levy O, Carrasco N. Post-transcriptional regulation of the sodium/iodide symporter by thyrotropin. *J Biol Chem* 2001;276:21458–63.
37. Wapnir IL, Greco RS, Dohan O, Amenta PS, Carrasco N. NIS expression in thyroid cancers. *Proc Am Soc Clin Oncol* 2001;20:336B.
38. Dohan O, Baloch Z, Barnevi Z, Livolsi V, Carrasco N. Predominant intracellular overexpression of the Na⁺/I⁻ symporter in a large sampling of thyroid cancer cases. *J Clin Endocrinol Metab* 2001;86:2697–700.
39. Kogai T, Schultz JJ, Johnson LS, Huang M, Brent GA. Retinoic acid induces sodium/iodide symporter gene expression and radioiodide uptake in the MCF-7 breast cancer cell line. *Proc Natl Sci USA* 97:8519–24.
40. Tanosaki S, Ikezoe T, Heaney A, et al. Effect of ligands of nuclear hormone receptors on sodium/iodide symporter expression and activity in breast cancer cells. *Breast Cancer Res Treat* 2003;79:335–45.
41. Kogai T, Kanamoto Y, Che LH, et al. Systemic retinoic acid treatment induces sodium/iodide symporter expression and radioiodide uptake in mouse breast cancer models. *Cancer Res* 2004;64:415–22.
42. Samaan N, Schultz P, Haynie T, Ordonez N. Pulmonary metastasis of differentiated thyroid carcinoma: treatment results in 101 patients. *J Clin Endocrinol Metab* 1985;60(2):376–80.
43. Schlumberger M, Tubiana M, De Vathaire F, et al. Long-term results of treatment of 283 patients with lung and bone metastases from differentiated thyroid carcinoma. *J Clin Endocrinol Metab* 1986;63:960–7.
44. Dadachova E, Bouzazhah B, Zuckier LS, Pestell RG. Rhenium-188 as an alternative to iodine-131 for treatment of breast tumors expressing the sodium/iodide symporter (NIS). *Nucl Med Biol* 2002;29:13–8.
45. Dadachova E, Carrasco N. The Na/I symporter (NIS): imaging and therapeutic applications. *Semin Nucl Med* 2004;34:23–31.
46. Maxon HR, Schroder LE, Washburn LC, et al. Rhenium-188 (Sn)HEDP for treatment of osseous metastases. *J Nucl Med* 1998;39:659–63.
47. Hoher M, Wohrle J, Wohlfrom M, et al. Intracoronary β -irradiation with a rhenium-188-filled balloon catheter: a randomized trial in patients with *de novo* and restenotic lesions. *Circulation* 2003;107(24):3022–5.
48. Press O, Eary JF, Petersdorf SH, et al. Phase II trial of ¹³¹I-B1 (anti-CD20) antibody therapy with autologous stem cell transplantation for relapsed B-cell lymphomas. *Lancet* 1995;346:336–40.
49. Liu SY, Eary JF, Petersdorf SH, et al. Follow-up of relapsed B-cell lymphoma patients treated with iodine-131-labeled anti-CD20 antibody and autologous stem-cell rescue. *J Clin Oncol* 1998;16(10):3270–8.
50. van Santen H, Kraker J, van Eck B, de Vijlder JJ, Vulmsa T. High incidence of thyroid dysfunction despite prophylaxis with potassium iodide during ¹³¹I-meta-iodobenzylguanidine treatment in children with neuroblastoma. *Cancer (Phila.)* 2002;94:2081–9.
51. Dillman R. Radiolabeled anti-CD20 monoclonal antibodies for the treatment of B-cell lymphoma. *J Clin Oncol* 2002;20:3545–57.
52. Carrasco N. Iodide transport in the thyroid gland. *Biochim Biophys Acta* 1993;1154:65–82.
53. van Santen H, Kraker J, van Eck B, de Vijlder JJ, Vulmsa T. Improved radiation protection of the thyroid gland with thyroxine, methimazole, and potassium iodide during diagnostic and therapeutic use of radiolabeled metaiodobenzylguanidine in children with neuroblastoma. *Cancer (Phila.)* 2003;98:389–96.